Synthesis and application of ^{131}I-fulvestrant as a targeted radiation drug for endocrine therapy in human breast cancer

GUOBING YIN[1], BIN ZENG[2], ZHIPING PENG[3], YING LIU[2], LU SUN[2] and CHANGAN LIU[4]

[1]Department of Breast, Thyroid, Pancreatic Surgery, The Second Affiliated Hospital of Chongqing Medical University; [2]Graduate School, Chongqing Medical University, Chongqing 400010; [3]Department of Radiological Medicine and Oncology, College of Basic Medicine, Chongqing Medical University, Chongqing 400016; [4]Department of Hepatobiliary Surgery, The Second Affiliated Hospital of Chongqing Medical University, Chongqing 400010, P.R. China

Received June 24, 2017; Accepted January 2, 2018

DOI: 10.3892/or.2018.6212

Abstract. The aim of this study was to label fulvestrant (an endocrine therapy drug for breast cancer) with radioiodine and to evaluate the effect of ^{131}I-fulvestrant on inhibiting the growth of human breast cancer and its influence on major organs in nude mice. Fulvestrant was labeled with radioiodine using a modified chloramine T method, and its chemical properties were assessed using traditional methods. The binding affinity of ^{131}I-fulvestrant was measured by radioligand binding assays, and its antiproliferative activity was determined by MTT assays. The ability of ^{131}I-fulvestrant to kill MCF-7 and MDA-MB-231 cells was also detected by MTT assays. We established MCF-7 cell xenografts in nude mice and monitored tumor growth and critical organ function. When the labeling reactions were conducted for 5 min at room temperature at pH 7.5, the radiochemical yield of the ^{131}I labeling to fulvestrant was 62.34±1.8%, the radiochemical purity was 98.6±3.4%, and the half maximal inhibitory concentration (IC_{50}) at 48 h was 35 μCi. ^{131}I-fulvestrant was stable, and its binding affinity to estrogen receptor-positive (ER^+) MCF-7 cells was also retained. In addition, ^{131}I-fulvestrant exhibited similar cytotoxicity in MCF-7 and MDA-MB-231 cells, although MCF-7 cells showed a slightly more pronounced response. ^{131}I-fulvestrant continuously exerted a tumor suppressive effect on MCF-7 cells but not on MDA-MB-231 cells ($P<0.05$). Upon intravenous injection of ^{131}I-fulvestrant into nude mice, the radioactivity distribution corresponded to ER expression patterns and was primarily confined to the tumor. ^{131}I-fulvestrant exhibited a precise growth inhibition effect on MCF-7 breast cancer cells, and its effects on general conditions of nude mice and their major organs were manageable. Therefore, radioiodine labeling of fulvestrant was successful and could be used to develop novel drugs for breast cancer by superimposing the benefits of radiotherapy and endocrine therapy.

Correspondence to: Dr Ying Liu, Graduate School, Chongqing Medical University, 74 Linjiang Road, Yuzhong, Chongqing 400010, P.R. China
E-mail: vitasqian@sina.com

Key words: adioiodine (^{131}I), fulvestrant, improved chloramine T method, ^{131}I-fulvestrant, breast cancer cells, xenografts, growth inhibition

Introduction

Radioactive iodine (^{131}I) has been used to treat differentiated thyroid carcinoma (DTC) for decades (1), and satisfactory results have been achieved. The sodium iodide symporter (NIS) is expressed in DTC cell membranes and can specifically transport ^{131}I into cells. Thus, ^{131}I is an ideal targeted internal radiotherapy that primarily produces beta rays to mimic radiotherapy. Furthermore, ^{131}I exerts little damage to surrounding tissues and causes fewer side effects (2-6).

Breast cancer comprises 33% of all cancer cases among women and is responsible for 19% of all cancer-related deaths (7). Improving the survival rate and quality of life for individuals suffering from breast cancer is of particular interest but has proven to be difficult (8). When advanced breast cancer metastasizes to the liver, cancer cells often exhibit chemotherapeutic and endocrine drug resistance (9,10). Surgery, chemotherapy, radiotherapy and endocrine therapy cannot effectively prevent such advanced cancer, and treatments often fail. Thus, we questioned whether ^{131}I can be used to treat breast cancer to improve patient outcomes.

The specific absorption and binding affinity of ^{131}I are exclusive to the thyroid *in vivo*. Breast cancer cells are unable to specifically absorb ^{131}I. Thus, fully replicating ^{131}I treatment of DTC in breast cancer is impractical. However, based on recent progress, the feasibility of incorporating ^{131}I into breast cancer treatment was examined as follows.

Relationship among estrogen, estrogen receptors and breast cancer. Most breast cancers are hormone-dependent, and estrogen receptors (ERs) are widely expressed in cancer cells and on cell membranes. Estrogen can specifically bind with ERs *in vivo* and promote tumor cell growth via a post-receptor effect. This ligand-receptor binding reaction has high specificity (11,12), and endocrine therapies that target ER-positive(ER^+) breast cancers are considerably effective (13). Two common breast cancer-based endocrine therapies include

blocking ER activity and estrogen production via antagonism of ERs. Drugs with chemical structures similar to ERs can be used for competitive binding, although such interactions do not induce a post-receptor effect. In addition, such binding inhibits signal transduction cascades, which interferes with the metabolism and growth of cancer cells (14,15). Commonly used drugs include tamoxifen, toremifene, and fulvestrant (16). Fulvestrant was approved in the United States in 2002 and is primarily administered to postmenopausal women who suffer cancer progression after anti-estrogen therapy. Fulvestrant has become the first-choice endocrine therapy for breast cancer in patients who develop drug resistance to tamoxifen. Furthermore, fulvestrant exerts more powerful endocrine and anticancer effects than tamoxifen and has a 300-fold stronger affinity for ERs than tamoxifen.

Progress in chemical modification of drugs. Chemical modification refers to altering functional groups and maintaining not only the basic structures of a drug but also its physicochemical properties and biological effects. The most common chemical modification methods are the Iodogen method, which is the process of introducing iodine atoms into a compound, and the chloramine T method. These approaches can be used to label fulvestrant with ^{131}I.

Once ^{131}I-fulvestrant was successfully synthesized, we sought to evaluate whether the compound binds to ERs in hormone-dependent breast cancer cells. Thus, the aim of this study was to assess both the radiotherapeutic and endocrine therapeutic effects of ^{131}I-fulvestrant on breast cancer cells.

Materials and methods

Experimental materials

Main reagents and their preparation. Fulvestrant (Rongda Pharm & Chem Co., Ltd., Hangzhou, China) was prepared as previously described (17-20): 2 mg fulvestrant was dissolved in 1 ml ethanol at a final concentration of 2 g/l. Chloramine T and sodium metabisulfite were obtained from the Chengdu Kelong Chemical Reagent Factory (Chengdu, China). Chloramine T (2 mg) was dissolved in 1 ml of a 1:1 ethanol and PBS solution (0.05 mmol/l, pH 7.5), and 2 mg sodium metabisulfite was dissolved in 1 ml of a 1:1 ethanol and PBS solution (0.05 mmol/l, pH 7.5) at a final concentration of 2 g/l. A Na^{131}I solution [Chengdu Gaotong Isotope Co., Ltd. (CNNC), Chengdu, China], FN3 medium-speed chromatography paper (Beijing Worthful Technology Co. Ltd., Beijing, China), ER ELISA kit (Shanghai Yansheng Industrial Co., Ltd., Shanghai, China), propidium lodide (Shang Hai Haoran Biological Technology Co., Ltd., Shanghai, China), Annexin V-FITC apoptosis detection kit (Becton-Dickinson, Franklin Lakes, NJ, USA), SephadexG15 (Pharmacia Company), RMPI-1640 and serum-free medium (HyClone) were used in the experiments. MTT, DMSO, 100% ethanol, and PBS were all obtained in China.

Main instruments and equipment. The following equipment was used for the experiments: a microbench (SW-CJ-1F; Suzhou Jiangdong Precision Istrument Co., Ltd., Suzhou, China), a desk centrifuge (KA-1000/TGL-16G; Shanghai Precision Istrument Co., Ltd., Shangai, China), a constant temperature oven (MIR160; Sanyo, Osaka, Japan), an electronic balance (Librorael-200; Shimadzu Corporation, Kyoto, Japan), a vacuum desiccator (Christ/Alpha1-2; Marin Christ, Osterode, Germany), a carbon dioxide incubator (Thermo Scientific Forma CO_2; Thermo Scientific Fisher, Waltham, MA, USA), a liquid mass spectrometer (Agilent Technologies 6410, Triple Quad LC/MS; Agilent Technologies, Santa Clara, CA, USA), a gamma counter (SN-684; Shanghai Hesuo Rihuan Photoelectric Istrument Co., Ltd., Shangai, China), a radioactivity detector (RM905a; Furui Hengchuang Technology Co., Ltd., Beijing, China), a microvortex mixer (VXH-3; Shanghai Huxi Analysis Istrument Factory Co., Ltd., Shangai, China), and an ultraviolet spectrophotometer (UV-265; Shimadzu Corporation).

Cell lines and animals. MCF-7 and MDA-MB-231 cells were obtained from the Typical Culture Preservation Committee Cell Bank of the Chinese Academy of Sciences. Female Balb/c nude mice (21 days old) were acquired from the Laboratory Animal Center at Chongqing Medical University.

Experimental procedures

Fulvestrant radio-iodination using an improved chloramine T (Ch-T) method. Step one: In a common EP tube, 50 μl fulvestrant was mixed with 100 μl chloramine T. Then, 1 mCi Na^{131}I was added to the tube, which was mixed via rapid oscillation and incubated at room temperature for 5 min. Step two: Sodium metabisulfite (200 μl) was added to the tube to terminate the iodination reaction. Referring to the methods described by Wang *et al* (21), the reaction was incubated at room temperature at pH 7.5 for 5 min and repeated 5 times.

Labeling rate detection by paper chromatography. Chromatography paper was cut into a 1x20-cm section and longitudinally folded. After centrifugation, the supernatant and Na^{131}I solution were suctioned using a capillary tube until 1 cm of liquid remained. After drying, the bottom of the paper was placed in ethanol approximately 0.5 cm deep and covered with a 2000-ml beaker. The chromatography paper was removed when the front edge of the spreading agent reached 10 cm from the sample point. After drying the chromatography paper at 37˚C in an oven, the paper was cut into 0.5-cm strips beginning at 1 cm from the bottom. The radioactivity (cpm) of the paper strips was detected by γ counter, and the labeling rate was determined from the following equation:

$$\text{Labeling rate} = \frac{\text{Radioactivity of the marker's paper}}{\text{Radioactivity of all paper strips}} \times 100\%$$

Separation and purification using molecular sieve chromatography. Sephadex G15 dextran gel was used as the solid phase, and 100% ethanol was the eluent. The outflow rate was 0.5 ml/min, and 10 drops of effluent were collected per test tube. The radioactivity (cpm) of the effluent was immediately detected, and the effluent with the highest radioactivity was defined as tube A.

Detection of ^{131}I-fulvestrant using mass spectrography. Fulvestrant powder (1 mg) was dissolved in 500 μl methanol solution, and 20 μl of the solution was removed to detect unlabeled fulvestrant. Another 50 μl of the fulvestrant solution

was removed after the iodination reaction, supplemented with pure water, and centrifuged at 15000 rpm. The supernatant was discarded, and 200 μl methanol was added to dissolve the precipitate. Then, 20 μl of this solution was used for mass spectrography.

^{131}I-fulvestrant stability detection by paper chromatography. Samples of tube A were collected at 24, 48, 72, 96, and 120 h after incubation at room temperature and were assessed using paper chromatography. The paper was cut into 1-cm strips, and the radioactivity (cpm) of these fragments was detected. The Na^{131}I and original reactive solution groups were established as control groups, and the radiochemical purity of all the samples was calculated concurrently using the following equation:

$$\text{Radiochemical purity} = \frac{\text{Radioactivity of the labeled compound}}{\text{Total radioactivity}} \times 100\%$$

Detection of ^{131}I-fulvestrant binding to ER using the cell binding assay. ER$^+$ MCF-7 cells were routinely cultured on a 24-well plate, and the culture medium was removed when growth reached approximately 50% confluency. Afterward, 1 ml serum-free medium was added to each well with 6 different concentrations (0.5, 1, 2, 4, 8, and 16 μCi) of ^{131}I-fulvestrant, and each concentration was tested in triplicate. After the cells were cultured for 24 h, the culture medium and cells were collected in order based on the concentration added, and radioactivity was detected.

Growth inhibition of ^{131}I-fulvestrant-treated MCF-7 and MDA-MB-231 cells as assessed via MTT assays. Group A: MCF-7 cells (1000 per well) were seeded into four 96-well plates. Four different concentrations of ^{131}I-fulvestrant (10, 20, 40, and 80 μCi) were added to each well in triplicate. A blank control and negative control treatment were also included on each plate, and one 96-well plate was removed every 24 h to measure cell proliferation. Group B: MDA-MB-231 cells underwent the same treatments as described for group A. Group C: MCF-7 cells ($5x10^5$ cells in 4 ml) were evenly aliquoted into 4 sterile centrifuge tubes. First, 0, 1, 3, or 7 ml of serum-free medium was added to the tubes followed by the addition of 0, 20, 40, or 80 μCi of ^{131}I-fulvestrant. After 1 h, the cells were centrifuged at 1000 rpm, and the supernatant was removed. The cells were then washed with PBS, resuspended in 2.4 ml ordinary culture medium and measured as described for group A. Group D: MDA-MB-231 cells underwent the same treatments as described for group C.

Coloration: One 96-well plate was removed every 24 h, and 20 μl MTT solution (5 mg/ml) was added to each well. After a 4 h of incubation, the culture medium was gently removed, and 150 μl DMSO was added to each well. The plate was then placed on a shaker for 10 min. The absorbance (A) at 490 nm was measured using an enzyme-linked immunometric meter. Blank wells were set as zero, and the negative control group was established to calculate the inhibition rate as follows:

$$\text{Inhibition rate}(\%) = (1 - \frac{A_{490} \text{ of experimental group}}{A_{490} \text{ of blank group}}) \times 100\%$$

Growth inhibition of ^{131}I-fulvestrant-treated MCF-7 cells as assessed via flow cytometry. MCF-7 cells were treated with ^{131}I-fulvestrant at different concentrations (10, 20, 40, 80 μCi) and tested at 24, 48, 72 and 96 h. The negative control group and the blank control group were analyzed after dyeing with Annexin V-FITC and propidium iodide.

Establishment of MCF-7 cell xenografts (22,23). A single-cell suspension of MCF-7 cells (0.5 ml, $2x10^6$/ml) was subcutaneously injected into the right shoulders of 21-day-old female Balb/c nude mice. These nude mice were maintained in an independent ventilation cage (IVC) system within a clean level barrier animal facility.

Distribution of ER in critical organs and xenografts of nude mice detected by immunohistochemistry. Three female xenograft nude mice without any other intervention were euthanized after inoculation with MCF-7 cells for 5 weeks, by which time xenografts had formed. Critical organs and xenografts were immediately removed and fixed in 10% formaldehyde. Referring to the methods described by Nishihara *et al* (24), immunohistochemistry was used to detect the ER distribution in these tissues.

Distribution of radionuclides in vivo and the effects of intravenous administration of ^{131}I-fulvestrant on xenograft tumors and organs

Whole-body ECT imaging of xenografts and radioactivity in organs. One hundred microliters of 200 μCi ^{131}I-fulvestrant was intravenously injected into mice. After 1 h, the mice were administered general anesthesia followed by ECT scanning with a detection time set at 300 sec. Two hours later, 1 ml blood was collected retro-orbitally. The nude mice were then euthanized, and their critical organs were immediately removed and weighed. Radioactivity of the blood and organs was detected.

Changes in xenograft tumors and organs after intravenous injection of ^{131}I-fulvestrant. Nine nude mice with xenografts were randomly divided into 3 groups, groups E-G, and the volume (length x width x height) of the xenografts was measured through the surface of the body. The mice received intravenous injections of 200 μCi ^{131}I-fulvestrant dissolved in 67% ethanol (group E, approximately 50 μl), 400 μCi ^{131}I-fulvestrant dissolved in 67% ethanol (group F, approximately 100 μl) or 100 μl 67% ethanol (group G). Tumor volumes were measured weekly, and the general conditions of the mice were observed daily. After 4 weeks, the mice were euthanized, and critical organs underwent H&E staining and were observed under a light microscope.

Changes in xenograft tumors after ^{131}I-fulvestrant injection into tumors. ^{131}I-fulvestrant (200 μCi) was injected into the core and basal regions of tumors in 3 nude mice. After 24 h, the mice were placed under general anesthesia and subjected to ECT scanning. After 1 week, changes in tumor size were observed, and 1 ml blood was collected retro-orbitally. The nude mice were then euthanized, and critical organs immediately were removed and weighed. Radioactivity of the blood and organs was detected.

Statistical analysis. In this study, the measured data are expressed as the mean ± standard deviation (SD), and numerical

Table I. Radiochemical purity testing results (n=3).

	24 h	48 h	72 h	96 h	120 h
Radiochemical purity (%)	98.65±3.43	97.24±2.98	96.68±3.12	95.52±3.36	93.47±4.32

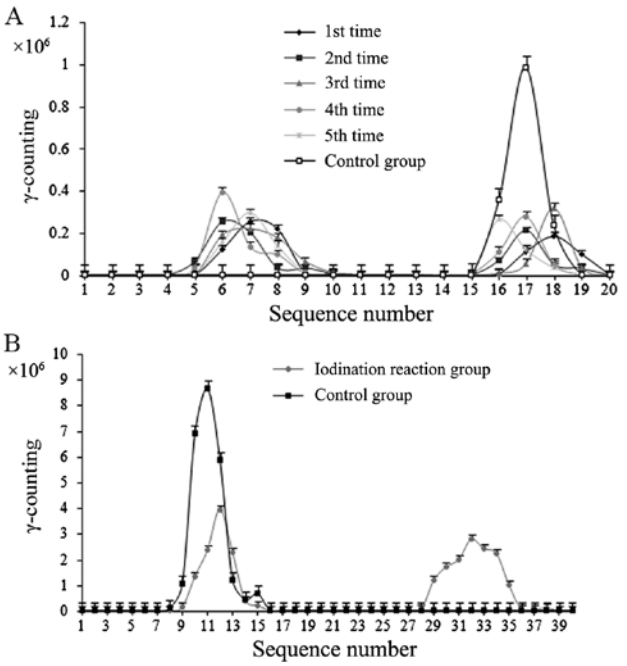

Figure 1. (A) Paper chromatographic results of the ^{131}I labeled compound and Na^{131}I control groups (n=5). (B) Results of molecular sieve chromatography (n=5).

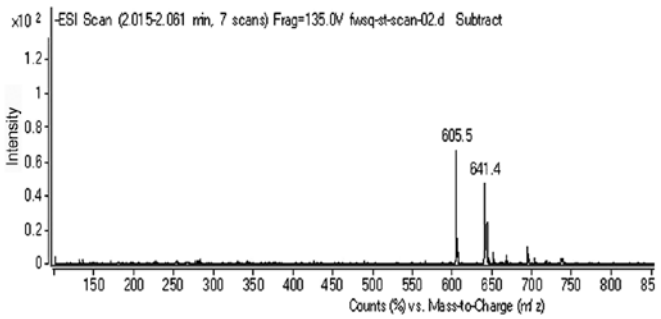

Figure 2. Mass spectrogram of the compounds produced from the iodination reaction (n=3).

data are expressed as rates. SPSS13.0 statistical software was used for statistical tests. The measured data were statistically analyzed using either the t-tests or analysis of variance, and significance level was set at α=0.05.

Results

Radioactivity of the ^{131}I labeled compound and Na^{131}I control groups. The iodination reaction generated a compound labeled with ^{131}I, and the labeling rate was 60.56±1.2% (Fig. 1A).

Separation and purification results. Gamma counting of the iodination reaction using the eluate from molecular sieve chromatography revealed a double peak (Fig. 1B). The first peak was consistent with the position of the iodine peak of the control group and was confirmed as iodine. The labeling rate was 62.34±1.8%, which was similar to the results of the paper chromatography assessment. Thus, purified iodide was collected.

Mass spectrometry analysis using a liquid mass spectrometer. The molecular weight of ^{131}I is 131 (Fig. 2), and ^{131}I showed a peak at 130.9 (which was knocked down from ^{131}I-fulvestrant). The molecular weight of fulvestrant is 606.77, and fulvestrant showed a peak at 605.5. Additionally, ^{131}I-fulvestrant presented a peak at 737.7. Because of the negative ion detection, one hydrogen atom should be added to the molecular weight, thus yielding 737.4 - 606.77 + 1 = 131.93. It can be inferred that an iodide atom was successfully attached to fulvestrant after the iodination reaction.

Detection of ^{131}I-fulvestrant stability. The iodination reaction products at 24, 48, and 72 h (Fig. 3) showed a single peak. There was a weak second peak at 96 h, which was increased at 120 h. The first peak in the control groups (Na^{131}I group and the original reactive solution group) corresponded to stable ^{131}I-fulvestrant, and the second peak corresponded to iodine (^{131}I). The second peak appeared in the range of iodine in the chromatographic band, similar to the band observed in the control group (Na^{131}I). These data indicate that ^{131}I-fulvestrant was stable for 72 h and began to decay at 96 h, which suggests that ^{131}I-fulvestrant maintains a stable chemical structure for 120 h after generation. Radiochemical purity greater than 95% within 96 h after the iodination reaction revealed that ^{131}I-fulvestrant was stable (Table I).

Binding affinity of ^{131}I-fulvestrant in ER$^+$ MCF-7 cells. ^{131}I-fulvestrant can bind to ER$^+$ MCF-7 cells, but the binding affinity did not increase with increasing concentrations of ^{131}I-fulvestrant (Fig. 4A); rather, the binding peaked and saturated at a dose of 4 μCi. In addition, the amount of bound ligand slightly decreased with increasing doses. There was no significant difference between these two groups (F=9.03, P=0.12).

Effect of ^{131}I-fulvestrant on growth inhibition of ER$^+$ MCF-7 cells. The survival of ER$^+$ MCF-7 cells was assessed at various time points after treatment with different doses of ^{131}I-fulvestrant (Fig. 4B). There were significant differences among all the groups (F=14.02, P=0.00), which indicated that with increasing radiation doses and incubation times, the number of surviving cells decreased, thus reflecting a marked inhibitory effect. In addition, none of the groups reached a

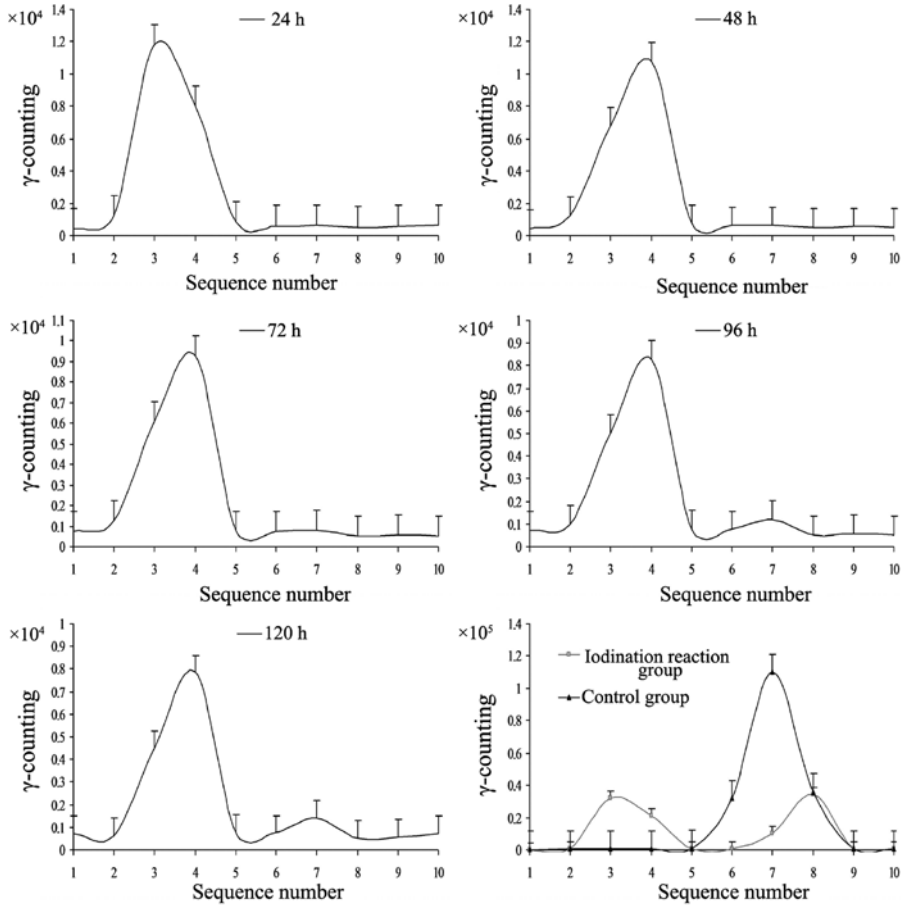

Figure 3. Paper chromatographic consequences of the control group and after 24, 48, 72, 96, and 120 h (n=5).

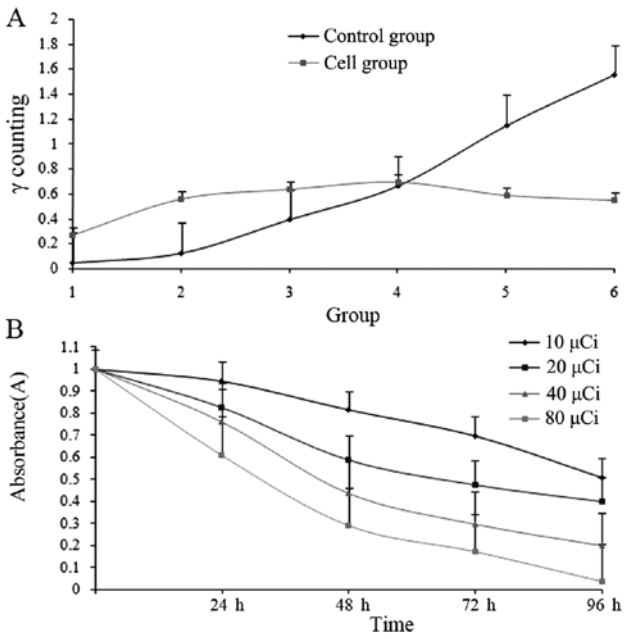

Figure 4. (A) Detection of the binding affinity of ^{131}I-fulvestrant with ER$^+$ MCF-7 cells (n=3) (F=9.03, P=0.12). (B) Growth inhibition curve of ^{131}I-fulvestrant in ER$^+$ MCF-7 cells (n=3) (F=14.02, P=0.00).

measurable half maximal inhibitory concentration (IC_{50}) at 24 h, whereas at 48, 72, and 96 h, the IC_{50} values were 35, 18, and 13 μCi, respectively.

Inhibitory effects of different concentrations of ^{131}I-fulvestrant on the growth of human breast cancer cells. In Table II, there was a significant difference between each concentration ($P<0.05$) within groups A and B, reflecting marked inhibition, but there was no significant difference between groups A and B ($P>0.05$). Group C showed weaker inhibition with persistent ^{131}I-fulvestrant treatment than groups A and B. After 1 h, ^{131}I-fulvestrant exposure to MDA-MB-231 cells was halted in group D, the radiation damage was terminated, and growth inhibition at each concentration was diminished and did not reach the IC_{50} values. However, there were significant differences in group D compared with groups A-C.

Results of growth inhibition of ^{131}I-fulvestrant-treated MCF-7 cells as assessed via flow cytometry. After treating with different concentrations of ^{131}I-fulvestrant (10, 20, 40, and 80 μCi), the apoptosis rates of MCF-7 cells were detected at 24, 48, 72 and 96 h. The results are shown in Fig. 5. Flow cytometry revealed that the apoptosis rate and the cell necrosis rate increased with increasing doses and durations of ^{131}I-fulvestrant treatment. A significant dose-time dependence was found, which was consistent with the MTT assay. The mechanism included both induction of apoptosis and cell necrosis caused by cytotoxicity.

Animal model. Of the 15 nude mice inoculated, 14 successfully grew xenografts after 4-6 weeks, which corresponds to a one-time success rate of 93.33%. The lone nude mouse that

Table II. Inhibition of ^{131}I-fulvestrant on the growth of MCF-7 and MDA-MB-231 cells (mean ± SD, n=3).

Group	10 μCi (absorbance)	20 μCi (absorbance)	40 μCi (absorbance)	80 μCi (absorbance)
Group A				
24 h	0.945±0.062	0.813±0.045	0.696±0.056	0.509±0.046
48 h	0.826±0.048	0.586±0.037	0.473±0.034	0.396±0.019
72 h	0.763±0.033	0.437±0.026	0.297±0.042	0.197±0.025
96 h	0.612±0.042	0.288±0.017	0.169±0.009	0.033±0.002
Group B				
24 h	0.965±0.012	0.828±0.017	0.736±0.062	0.582±0.035
48 h	0.876±0.023	0.643±0.025	0.547±0.057	0.369±0.028
72 h	0.812±0.048	0.512±0.067	0.435±0.074	0.235±0.032
96 h	0.824±0.032	0.303±0.054	0.281±0.046	0.068±0.017
Group C				
24 h	0.954±0.021	0.908±0.025	0.832±0.031	0.795±0.025[a]
48 h	0.882±0.032	0.833±0.019	0.667±0.014	0.626±0.017[a]
72 h	0.816±0.043	0.676±0.017[a]	0.553±0.018[a]	0.525±0.024[a]
96 h	0.723±0.018	0.512±0.026[a]	0.418±0.022[a]	0.391±0.019[a]
Group D				
24 h	0.972±0.022	0.965±0.015	0.943±0.011	0.835±0.023
48 h	0.956±0.019	0.934±0.017	0.876±0.024	0.768±0.022
72 h	0.923±0.056	0.907±0.025	0.828±0.016	0.742±0.016
96 h	0.908±0.025	0.862±0.029	0.811±0.025	0.715±0.031

[a]P<0.05 for respective time points.

Table III. ER-α expression in xenografts in nude mice and critical organs (mean ± SD, n=3).

Organs	Positive rate (%)	Strong positive rate (%)
Liver[a]	74.14±7.52	46.86±5.21
Xenografts[a]	68.33±6.45	44.57±5.37
Thyroid[a]	54.76±4.88	41.45±2.32
Kidney[a]	64.45±5.76	40.46±2.79
Lung[a]	68.23±3.79	43.65±2.18
Small intestine[b]	27.24±2.12	5.24±0.46
Heart[b]	22.25±1.58	8.66±0.67

[a]Group E; [b]group F.

did not grow a xenograft was inoculated with 2x10^6/ml MCF-7 cells a second time, and xenografts were successfully detected 4 weeks later. Xenografts were used for experiments when their diameter reached approximately 1 cm.

Results of the distribution of ERs in critical organs and xenografts of nude mice under light microscopy. Immunohistochemical staining of critical organs and xenografts was carried out (Fig. 6). As shown in the Fig. 6, the positive rate and the strong positive rate of ER-α in the xenografts, liver, lung, thyroid and kidney were high, while they were low in cardiac muscle and small intestine. The positive rate and the strong positive rate were analyzed by IPP 6.0 software, and the results are shown in Table III.

There was no significant difference in the positive rate of ER-α between each organ within group E (P>0.05), and there was a significant difference in the positive rate of ER-α between groups E and F (P<0.05). The *in vivo* expression of ER-α in nude mice with MCF-7 cell xenografts was not significantly different than the ER expression of MCF-7 cells *in vitro*. Thus, ER-α was expressed in all of the detected tissues; the highest expression was observed in liver and the lowest in small intestine.

Radionuclide distribution in vitro after ^{131}I-fulvestrant intravenous injection. At 2 h after intravenous injection of ^{131}I-fulvestrant, radioactivity in the blood peaked and corresponded to 20.76±2.54%, whereas the percentage of radioactivity in the remaining organs was low (Table IV).

ECT whole-body imaging of nude mice with xenografts. Radionuclide imaging was observed in tumors (Fig. 7, left), and radioactivity in the chest and abdominal organs was also found. However, no apparent activity in the thyroid was observed.

Changes in xenografts and organs after intravenous injection of ^{131}I-fulvestrant. In Table V, the tumor volume in group E gradually reduced within 2 weeks after ^{131}I-fulvestrant injection, but the volume recovered during the 3rd week. The

Table IV. Radioactivity of important organs *in vitro* (% ID/g, mean ± SD, n=3).

Organs	Organ weight (g)	Radioactivity concentration (μCi/g)	Total radioactivity (μCi)	Total radioactivity rate (%)
Tumor	1.15±0.16	5.79±0.31	6.67±0.42	4.33±0.28
Liver	2.8±0.22	4.74±0.52	13.28±1.15	8.62±0.47
Blood	1.2±0.04	26.64±2.88	31.97±3.11	20.76±2.54
Kidney	0.61±0.04	3.48±0.22	2.13±0.16	1.38±0.12
Heart	0.42±0.03	4.54±0.43	1.91±0.25	1.64±0.16
Lungs	1.26±0.02	3.08±0.27	3.88±0.28	2.52±0.21
Small intestine	1.68±0.12	5.16±0.52	8.67±0.65	3.63±0.43
Thyroid	0.18±0.01	4.02±0.33	0.72±0.08	1.47±0.16

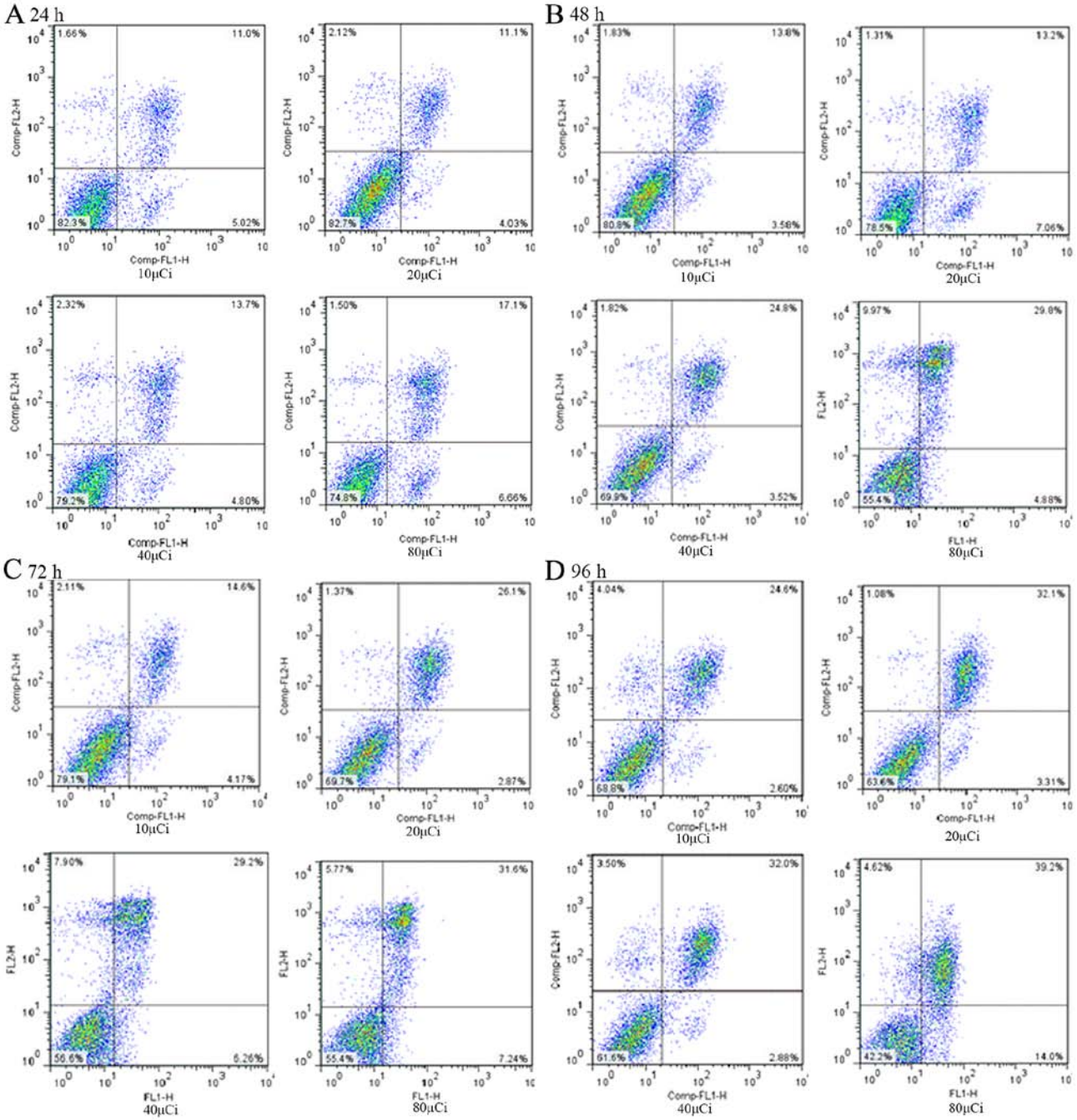

Figure 5. Flow cytometry results of apoptosis at 24 h (A), 48 h (B), 72 h (C) and 96 h (D).

Table V. Changes in tumor volume after injection (mean ± SD, n=3).

Group	0 (cm^3)	1 week (cm^3)	2 weeks (cm^3)	3 weeks (cm^3)	4 weeks (cm^3)
Group E	1.24±0.21[a]	1.04±0.15[b]	0.85±0.13[b]	0.92±0.14[b]	1.06±0.12[b]
Group F	1.35±0.25[a]	0.67±0.18[b]	0.52±0.09[b]	0.48±0.06[b]	0.69±0.08[b]
Group G	1.22±0.19[a]	1.34±0.26[b]	1.49±0.31[b]	1.62±0.35[b]	1.85±0.38[b]

[a]P>0.05, no significant difference, [b]P<0.05, a significant difference.

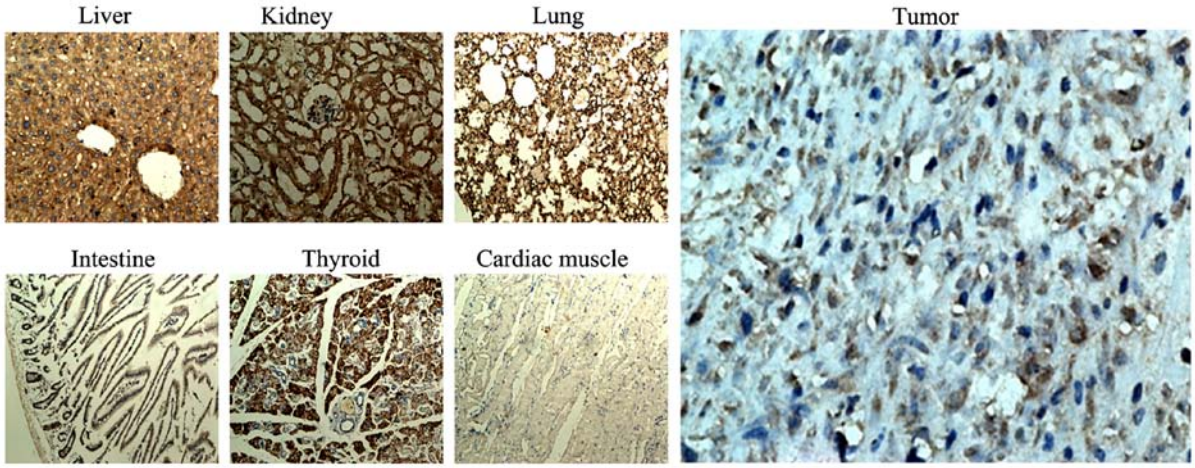

Figure 6. ER-α expression in tissues and xenografts in nude mice (IHC 10x20).

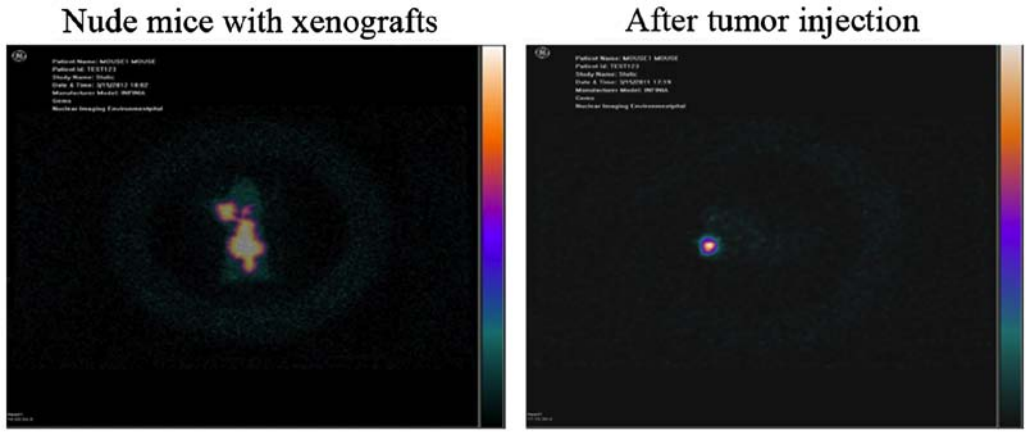

Figure 7. Left, ECT whole-body imaging of nude mice with xenografts. Right, ECT whole-body imaging of nude mice with xenografts after tumor injection.

tumor volume in group F was gradually reduced within 3 weeks after injection but began to increase during the 4th week. However, group G maintained continuously increasing tumor growth.

General conditions and morphological changes in critical organs under light microscopy. Nude mice in all the groups tolerated the intravenous injection and survived. Mice in groups E and F exhibited anorexia and reduced activity the day after injection but returned the normal after approximately 3 days. No abnormal behaviors were observed in the mice in group G. After 4 weeks, H&E staining of the xenografts and organs was performed. The liver, lung, kidney, thyroid, heart, small intestine and other tissues did not exhibit obvious damage (Fig. 8), but the tumor tissue presented necrosis.

Xenograft changes and ECT imaging results after ^{131}I-fulvestrant injection into tumors

Xenograft changes. After ^{131}I-fulvestrant injection into the tumor site, 3 nude mice showed good tolerance with no significant changes in their general condition. Massive necrosis was observed in the MCF-7 cell xenografts, which indicated the effect of ^{131}I-fulvestrant against the tumors.

At 72 h after injection, the nude mice were sacrificed, and the xenografts were observed via H&E staining. The large-area

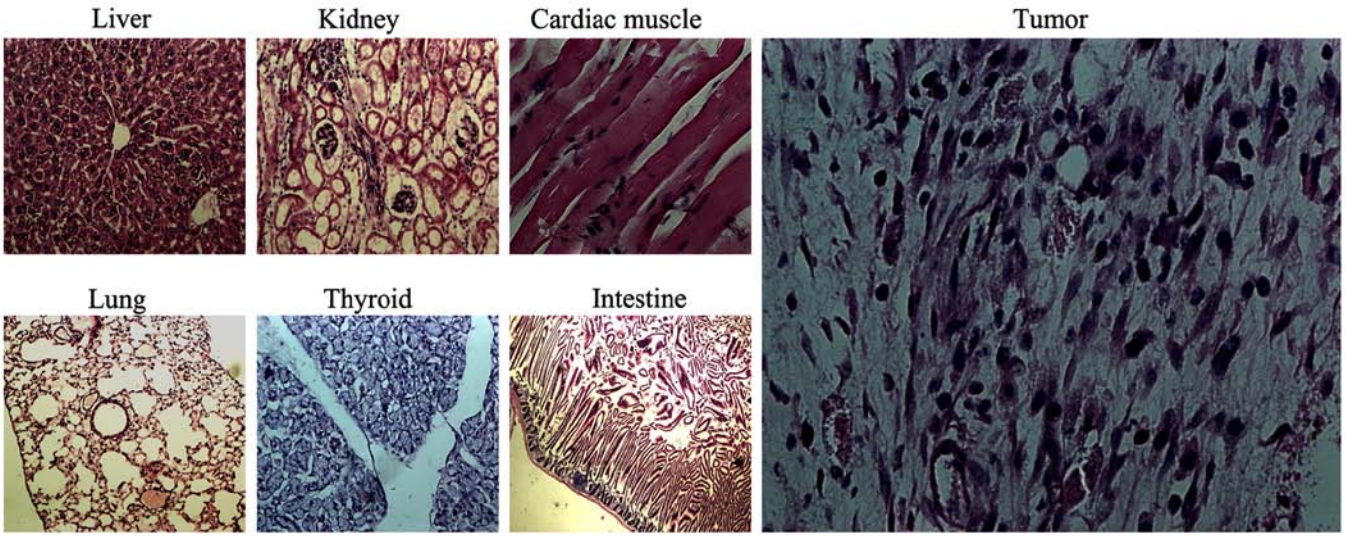

Figure 8. Top: Liver, kidney, and cardiac muscle tissue from nude mice treated with 400 μCi ^{131}I-fulvestrant (H&E 10x20). Bottom: ER-α expression in the lung, thyroid and intestinal tissues of nude mice (IHC 10x20). No anomalous changes were observed. Right: tumor cells from nude mice did not show signs of severe injury. However, the number of tumor cells was reduced in the peripheral area on the left; some cell nuclei disappeared, and the dye in cytoplasm was light in color. These observations indicated that these cells were either necrotic or close to necrosis (H&E 10x20).

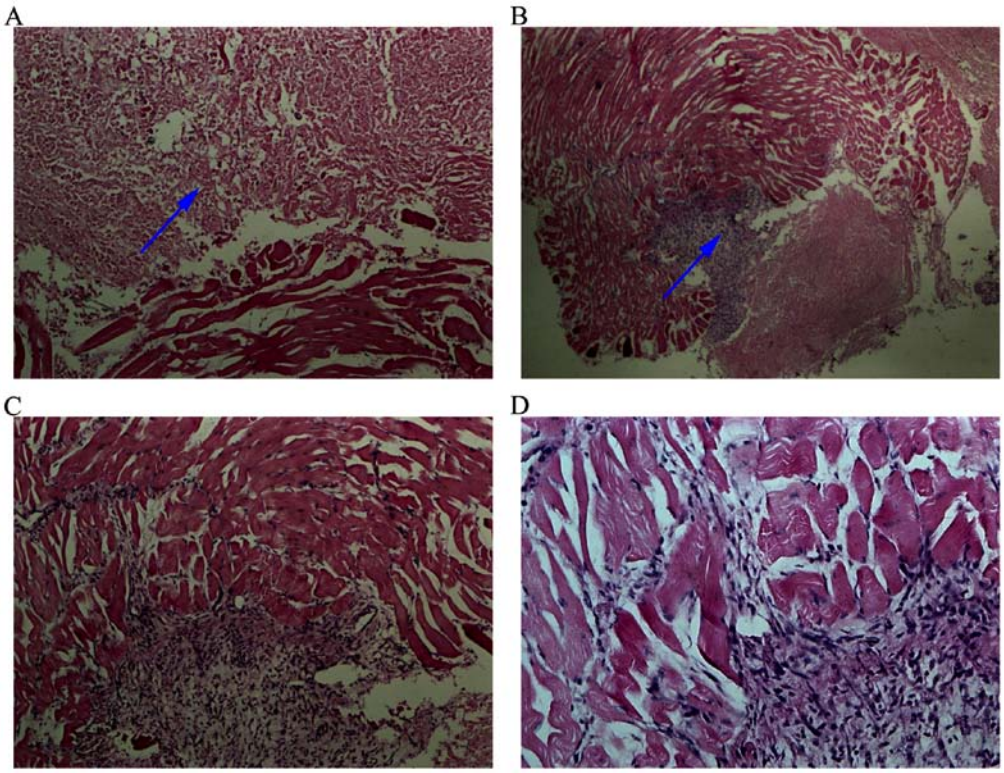

Figure 9. (A) Massive necrosis occurred in xenografts, but normal tissue did not present obvious injuries. (B) Tumor cells were visible near muscle tissue (arrow points), but the muscle tissue was not obviously injured. (C and D) MCF-7 cell xenografts in nude mice. (A and B) ^{131}I-fulvestrant treated MCF-7 cell xenografts; (C and D) MCF-7 cell xenografts without any intervention, H&E 10x20)

tumor nuclei had disappeared (Fig. 9), cell morphology was altered, and the xenografts appeared as amorphous homogeneous red tissues. However, a few surviving MCF-7 cells were found in normal adjacent tissue.

ECT whole-body imaging of nude mice with xenografts after tumor injection. At 24 h after ^{131}I-fulvestrant injection at the tumor site, ECT scans showed that the radionuclide was primarily confined to the tumor site (Fig. 7, right) and did not spread to other parts of the body.

Discussion

To achieve targeted radiotherapy of malignant tumors, many new radiotherapies have been explored, including conformal radiotherapy, administration of radioactive particles,

radioactive iodine injection and monoclonal antibody technology. Among these, the most encouraging approach has been ^{131}I radiation therapy for differentiated thyroid carcinoma. In this approach, tumor cells actively absorb radioactive iodine, thus achieving targeted radiotherapy. In addition, ^{131}I primarily relies on beta rays to induce radiotherapy with a range of millimeters. Therefore, ^{131}I radiation therapy induces little damage to surrounding tissues while simultaneously overcoming the 'cross fire' radiotherapy of tumor cells, which is derived from heterogeneity in tumors that do not express ERs (2-5).

This study aimed to incorporate ^{131}I into breast cancer treatments. Under normal conditions *in vivo*, the specific absorption and binding affinity of ^{131}I have been exclusively studied in the thyroid. Therefore, ^{131}I must be bound to an appropriate carrier. An improved chloramine T method was used in this study based on chemical synthesis, which is a widely accepted approach for radioiodine labeling of proteins, polypeptides and other macromolecules. This study aimed to attach ^{131}I to fulvestrant, a small organic molecule with a weight of 606.77 and poor water solubility but high ethanol solubility. However, chloramine T and sodium metabisulfite have high water solubility but poor ethanol solubility. Thus, radio-iodination cannot be implemented using the traditional chloramine T method because all the substances are aqueous, and thus, a modified chloramine T method was implemented. Fulvestrant was dissolved in ethanol, and chloramine T and sodium metabisulfite were dissolved in 50% ethanol. Therefore, the final ethanol concentration in the iodination reaction system was 70%. This not only ensures the dissolution of all the substances but also allows chloramine T to release perchlorate radicals into the water to oxidize iodide to atomic iodine.

This study showed that stable labeling of fulvestrant with ^{131}I could be implemented using an improved chloramine T method. The radiochemical yield of radioiodine labeling to fulvestrant was 62.34±1.8%, which was detected using paper chromatography and molecular sieve chromatography. ^{131}I-fulvestrant had a stable chemical structure as reflected by the results that the iodine moiety did not dissociate from fulvestrant 72 h after labeling and was subsequently released slowly. The results of the cell binding assay demonstrated that ^{131}I-fulvestrant could also interact with estrogen-dependent breast cancer cells and exhibited saturation, consistent with traditional ligand-receptor binding theory. Increasing doses slightly decreased the amount of bound ligand, which we interpreted as increased radiation damage to breast cancer cells with higher radiation doses. It should further be elucidated whether radiation damage in breast cancer cells is related to decreased expression of estrogen at the molecular level.

In breast cancer, ER expression is an important marker of prognosis and primarily serves as a predictor of patient responses to endocrine therapy, individuals who have ER$^+$ tumors are more likely to exhibit a better response and prognosis than those with ER$^-$ tumors (25). Human breast cancer MCF-7 cells (ER$^+$, estrogen receptor-positive) and MDA-MB-231 cells (ER$^-$, estrogen receptor-negative) were selected for this investigation, because these two cell lines represent ER$^+$ and ER$^-$ breast cancer cells. Thus, we selected these two cell lines for this experiment. Several studies have shown that MCF-7 cells either overexpress or can induce overexpression of ER-α (26-29).

Breast cancer cells express the NIS (30), which uses the transmembrane sodium ion concentration gradient as the primary driving force to transport iodine into cells (31-33). Therefore, this protein provides a new target for improving radioiodine treatment of breast cancer.

The results of the MTT assay showed that the growth of these two types of breast cancer cells was inhibited by ^{131}I-fulvestrant. Transient contact experiments showed that the growth inhibition of breast cancer cells was decreased, and this effect was significantly more pronounced in MCF-7 cells than in MDA-MB-231 cells. Provided that a specific dose of radiation is present in the culture medium, we suggest that MCF-7 and MDA-MB-231 cells will be subjected to radiation damage and growth inhibition regardless of ER-α expression status. When the radioactive substance was removed, MDA-MB-231 cells were completely unaffected by the radioactive environment due to their inability to absorb ^{131}I-fulvestrant. However, ^{131}I-fulvestrant remained bound to ERs in MCF-7 cells and, thus, continued to cause radiation damage. This effect by which ^{131}I-fulvestrant induces tumor cell death represents a combination of radiotherapy and endocrine therapy.

MCF-7 cells either overexpress or can induce the overexpression of ER-α (26-29); concurrent with this, ER-α has a characteristically wide distribution throughout the body (34-36). Fulvestrant has fewer side effects and is regarded as a pure endocrine therapy-based antagonist of breast cancer. Studies have shown that fulvestrant can even downregulate ER expression; however, the mechanism of this activity is unclear (15,18,20).

After intravenous injection of ^{131}I-fulvestrant, the growth of the xenografts in nude mice was first reduced but later restored, which suggests that growth inhibition by ^{131}I-fulvestrant is due to a combination of radiotherapy and endocrine therapy. Growth recovery was subsequently shown to be related to the decrease in drug concentration *in vivo*, including the decay of radioiodine and the biological metabolism of fulvestrant. Nude mice with xenografts initially presented anorexia and reduced activity following ^{131}I fulvestrant injection. Tumor exhibited growth inhibition and tissue necrosis, but no significant organ damage was found upon morphological examination. This dichotomy is due to the fact that tumor cells and normal cells have different sensitivities to radiation, as tumor cells are more susceptible to radiation damage and have an inferior damage response compared to normal tissue cells.

Massive necrosis occurred in the tumors after ^{131}I-fulvestrant injection to the tumor site, and only a few residual tumor cells were found in normal adjacent tissues. ECT scanning showed that the radionuclide was primarily localized to the tumor site and did not spread to other parts of the body. It is understood that ^{131}I-fulvestrant maintains the poor aqueous solubility of fulvestrant. Thus, after local injection, ^{131}I-fulvestrant locally precipitated into crystals, which resulted in a high dose of localized radiation that could maximize its ability to kill tumor cells. In addition, although the crystalline solid cannot enter blood circulation, it is still possible to change its physical location in the tissue space. Therefore, ^{131}I-fulvestrant can be used to fight tumor cells over a larger local range. However, ECT scanning cannot be set to a different time point, and

the purpose of this experiment was to verify the effects of ^{131}I-fulvestrant. Once injected, ^{131}I-fulvestrant is slowly metabolized, and nude mice cannot tolerate a repeated injection. We plan to continue to investigate the *in vivo* pharmacokinetics of ^{131}I-fulvestrant on larger experimental animals (rabbits) in future studies.

Our goal was to prove that fulvestrant is stable and is able to kill tumor cells. Adding fulvestrant to the cell culture medium will produce a precipitate. Fulvestrant inhibited the growth of tumor cells, in contrast to the active killing effect of ^{131}I fulvestrant on tumors. Thus, we did not set fulvestrant as a control group. The lack of the fulvestrant control group was a limitation of our investigation. We plan to continue to compare fulvestrant with ^{131}I-fulvestrant in future investigation.

In conclusion, fulvestrant can be successfully labeled with radioiodine using an improved chloramine T method. The obtained product ^{131}I-fulvestrant is chemically stable and retains its binding affinity to estrogen-dependent breast cancer cells. ^{131}I-fulvestrant can precisely inhibit the growth of estrogen-dependent breast cancer cells via the following mechanisms: i) ^{131}I radiation damage to MCF-7 cells via delivery of ^{131}I-fulvestrant; ii) binding to ER, which blocks the tumorigenic effect of estrogen in MCF-7 cells; and iii) down-regulation of ER expression. Therefore, our investigation has made a significative exploration concerning the use of ^{131}I in the treatment of breast cancer, and lays the foundation to support patients who undergo ^{131}I treatment.

Acknowledgements

This research was supported by the Natural Science Foundation of Chongqing (grant no. cstc2012jjA10042) and the Chongqing Municipal Public Health Bureau (grant no. 2011-2-175).

References

1. Pitoia F and Miyauchi A: 2015 American thyroid association guidelines for thyroid nodules and differentiated thyroid cancer and their implementation in various care settings. Thyroid 26: 319-321, 2016.
2. Higashi T, Kudo T and Kinuya S: Radioactive iodine (^{131}I) therapy for differentiated thyroid cancer in Japan: Current issues with historical review and future perspective. Ann Nucl Med 26: 99-112, 2012.
3. Sawka AM, Straus S, Gafni A, Meiyappan S, David D, Rodin G, Brierley JD, Tsang RW, Thabane L, Rotstein L, *et al*: Thyroid cancer patients' involvement in adjuvant radioactive iodine treatment decision-making and decision regret: An exploratory study. Support Care Cancer 20: 641-645, 2012.
4. Haymart MR, Banerjee M, Stewart AK, Koenig RJ, Birkmeyer JD and Griggs JJ: Use of radioactive iodine for thyroid cancer. JAMA 306: 721-728, 2011.
5. Tuttle RM, Rondeau G and Lee NY: A risk-adapted approach to the use of radioactive iodine and external beam radiation in the treatment of well-differentiated thyroid cancer. Cancer Contr 18: 89-95, 2011.
6. Sacks W, Fung CH, Chang JT, Waxman A and Braunstein GD: The effectiveness of radioactive iodine for treatment of low-risk thyroid cancer: A systematic analysis of the peer-reviewed literature from 1966 to April 2008. Thyroid 20: 1235-1245, 2010.
7. Hosseinzadeh M, Eivazi Ziaei J, Mahdavi N, Aghajari P, Vahidi M, Fateh A and Asghari E: Risk factors for breast cancer in Iranian women: A hospital-based case-control study in tabriz, iran. J Breast Cancer 17: 236-243, 2014.
8. Howard-Anderson J, Ganz PA, Bower JE and Stanton AL: Quality of life, fertility concerns, and behavioral health outcomes in younger breast cancer survivors: A systematic review. J Natl Cancer Inst 104: 386-405, 2012.
9. Gradilone A, Raimondi C, Naso G, Silvestri I, Repetto L, Palazzo A, Gianni W, Frati L, Cortesi E and Gazzaniga P: How circulating tumor cells escape from multidrug resistance: Translating molecular mechanisms in metastatic breast cancer treatment. Am J Clin Oncol 34: 625-627, 2011.
10. Chen WJ, Wang H, Tang Y, Liu CL, Li HL and Li WT: Multidrug resistance in breast cancer cells during epithelial-mesenchymal transition is modulated by breast cancer resistant protein. Chin J Cancer 29: 151-157, 2010.
11. Dall G, Vieusseux J, Unsworth A, Anderson R and Britt K: Low dose, low cost estradiol pellets can support MCF-7 tumour growth in nude mice without bladder symptoms. J Cancer 6: 1331-1336, 2015.
12. Yang ZY, Wang MW, Zhang YP, Xu JY, Yuan HY and Zhang YJ: The biodistribution and imaging of 16α-(18F) fluroroestradiol (18F-FES) in rats and breast tumor-bearing nude mice. Shanghai Medical Imaging 20: 234-238, 2011.
13. Turner NC, Neven P, Loibl S and Andre F: Advances in the treatment of advanced oestrogen-receptor-positive breast cancer. Lancet 389: 2403-2414, 2017.
14. Dalmau E, Armengol-Alonso A, Muñoz M and Seguí-Palmer MÁ: Current status of hormone therapy in patients with hormone receptor positive (HR^+) advanced breast cancer. Breast 23: 710-720, 2014.
15. James R, Thriveni K, Krishnamoorthy L, Deshmane V, Bapsy PP and Ramaswamy G: Clinical outcome of adjuvant endocrine treatment according to Her-2/neu status in breast cancer. Indian J Med Res 133: 70-75, 2011.
16. Al-Mubarak M, Sacher AG, Ocana A, Vera-Badillo F, Seruga B and Amir E: Fulvestrant for advanced breast cancer: A meta-analysis. Cancer Treat Rev 39: 753-758, 2013.
17. Wardell SE, Nelson ER, Chao CA and McDonnell DP: Bazedoxifene exhibits antiestrogenic activity in animal models of tamoxifen-resistant breast cancer: Implications for treatment of advanced disease. Clin Cancer Res 19: 2420-2431, 2013.
18. Mishra AK, Abrahamsson A and Dabrosin C: Fulvestrant inhibits growth of triple negative breast cancer and synergizes with tamoxifen in ERα positive breast cancer by up-regulation of ERβ. Oncotarget 7: 56876-56888, 2016.
19. He S, Wang M, Yang Z, Zhang J, Zhang Y, Luo J and Zhang Y: Comparison of 18F-FES, 18F-FDG, and 18F-FMISO PET imaging probes for early prediction and monitoring of response to endocrine therapy in a mouse xenograft model of ER-positive breast cancer. PLoS One 11: e0159916, 2016.
20. Fernandes SA, Gomes GR, Siu ER, Damas-Souza DM, Bruni-Cardoso A, Augusto TM, Lazari MF, Carvalho HF and Porto CS: The anti-oestrogen fulvestrant (ICI 182,780) reduces the androgen receptor expression, ERK1/2 phosphorylation and cell proliferation in the rat ventral prostate. Int J Androl 34: 486-500, 2011.
21. Wang MH, Xu YJ, Wang ZZ, Liu M, Li Z, Weng W and Fan W: Radiolabeling of paclitaxel with ^{125}I. J Isotopes 21: 82-87, 2008.
22. Wang L, Mi C and Wang W: Establishment of lymph node metastasis of MDA-MB-231 breast cancer model in nude mice. Zhonghua Yi Xue Za Zhi 95: 1862-1865, 2015 (In Chinese).
23. Nofiele JT and Cheng HL: Establishment of a lung metastatic breast tumor xenograft model in nude rats. PLoS One 9: e97950-e97950, 2014.
24. Nishihara E, Nagayama Y, Inoue S, Hiroi H, Muramatsu M, Yamashita S and Koji T: Ontogenetic changes in the expression of estrogen receptor α and β in rat pituitary gland detected by immunohistochemistry. Endocrinology 141: 615-620, 2000.
25. Giacinti L, Giacinti C, Gabellini C, Rizzuto E, Lopez M and Giordano A: Scriptaid effects on breast cancer cell lines. J Cell Physiol 227: 3426-3433, 2012.
26. Liu L, Ma H, Tang Y, Chen W, Lu Y, Guo J and Duan JA: Discovery of estrogen receptor α modulators from natural compounds in Si-Wu-Tang series decoctions using estrogen-responsive MCF-7 breast cancer cells. Bioorg Med Chem Lett 22: 154-163, 2012.
27. Ko YM, Wu TY, Wu YC, Chang FR, Guh JY and Chuang LY: Annonacin induces cell cycle-dependent growth arrest and apoptosis in estrogen receptor-α-related pathways in MCF-7 cells. J Ethnopharmacol 137: 1283-1290, 2011.
28. Mendoza RA, Enriquez MI, Mejia SM, Moody EE and Thordarson G: Interactions between IGF-I, estrogen receptor-α (ERα), and ERβ in regulating growth/apoptosis of MCF-7 human breast cancer cells. J Endocrinol 208: 1-9, 2011.
29. Hong W, Chen L, Li J and Yao Z: Inhibition of MAP kinase promotes the recruitment of corepressor SMRT by tamoxifen-bound estrogen receptor alpha and potentiates tamoxifen action in MCF-7 cells. Biochem Biophys Res Commun 396: 299-303, 2010.

30. Kelkar MG, Senthilkumar K, Jadhav S, Gupta S, Ahn BC and De A: Enhancement of human sodium iodide symporter gene therapy for breast cancer by HDAC inhibitor mediated transcriptional modulation. Sci Rep 6: 19341, 2016.
31. Renier C, Do J, Reyna-Neyra A, Foster D, De A, Vogel H, Jeffrey SS, Tse V, Carrasco N and Wapnir I: Regression of experimental NIS-expressing breast cancer brain metastases in response to radioiodide/gemcitabine dual therapy. Oncotarget 7: 54811-54824, 2016.
32. Chatterjee S, Thaker N and De A: Combined 2-deoxy glucose and metformin improves therapeutic efficacy of sodium-iodide symporter-mediated targeted radioiodine therapy in breast cancer cells. Breast Cancer (Dove Med Press) 7: 251-265, 2015.
33. Poole VL and McCabe CJ: Iodide transport and breast cancer. J Endocrinol 227: R1-R12, 2015.
34. Jan KC, Ku KL, Chu YH, Hwang LS and Ho CT: Tissue distribution and elimination of estrogenic and anti-inflammatory catechol metabolites from sesaminol triglucoside in rats. J Agric Food Chem 58: 7693-7700, 2010.
35. Younes M and Honma N: Estrogen receptor β. Arch Pathol Lab Med 135: 63-66, 2011.
36. Ur Rahman MS and Cao J: Estrogen receptors in gastric cancer: Advances and perspectives. World J Gastroenterol 22: 2475-2482, 2016.